

Possible Relevance of the Allende Meteorite Conditions in Prebiotic Chemistry: An Insight into the Chondrules and Organic Compounds

Alejandro Heredia Barbero^{1*}, Héctor G. Vázquez López¹, Adriana L. Meléndez López¹, Jorge A. Cruz Castañeda¹, Daniel Luna Laviada^{1,2}, Karina E. Cervantes de la Cruz^{3,4*}, Victor Meza Laguna¹, Vladimir A. Basiuk¹, Ivonne Rosales Chávez⁵, Alicia Negrón Mendoza¹, Sergio Ramos Bernal⁴

¹Laboratorio de Evolución Química, Departamento de Química de Radiaciones y Radioquímica, Instituto de Ciencias Nucleares, Universidad Nacional Autónoma de México, Ciudad Universitaria, Ciudad de México, México

²Programa de Posgrado en Ciencias Químicas, Universidad Nacional Autónoma de México, Ciudad Universitaria, Ciudad de México, México

³Departamento de Física, Facultad de Ciencias, Carrera de Ciencias de la Tierra, Universidad Nacional Autónoma de México, Ciudad Universitaria, Ciudad de México, México

⁴Departamento de Física de Plasmas e Interacción de Radiación con Materia, Instituto de Ciencias Nucleares, Ciudad Universitaria, Ciudad de México, México

⁵Departamento de Física y Química Teórica, Facultad de Química, Universidad Nacional Autónoma de México, Ciudad Universitaria, Ciudad de México, México

Email: *aheredia@nucleares.unam.mx, luna.laviada@gmail.com, *karina-cervantes@ciencias.unam.mx, ivonne.rosales.ch@gmail.com, ramos@nucleares.unam.mx

How to cite this paper: Barbero, A.H., López, H.G.V., López, A.L.M., Castañeda, J.A.C., Laviada, D.L., de la Cruz, K.E.C., Laguna, V.M., Basiuk, V.A., Chávez, I.R., Mendoza, A.N. and Bernal, S.R. (2023) Possible Relevance of the Allende Meteorite Conditions in Prebiotic Chemistry: An Insight into the Chondrules and Organic Compounds. *Advances in Biological Chemistry*, 13, 82-99.

<https://doi.org/10.4236/abc.2023.133007>

Received: May 20, 2023

Accepted: June 23, 2023

Published: June 26, 2023

Abstract

The study of the mineral and organic content of the Allende meteorite is important for our understanding of the molecular evolution of the universe as well as the ancient Earth. Previous studies have characterized the magnetic minerals present in ordinary and carbonaceous chondrites, providing information on the evolution of magnetic fields. The interaction of organic compounds with magnetic minerals is a possible source of chemical diversity, which is crucial for molecular evolution. Carbon compounds in meteorites are of great scientific interest for a variety of reasons, such as their relevance to the origins of chirality in living organisms. This study presents the characterization of organic and mineral compounds in the Allende meteorite. The structural and physicochemical characterization of the Allende meteorite was accomplished through light microscopy, powder X-ray diffraction with complementary Rietveld refinement, Raman and infrared spectroscopy, mass spectrometry, scanning electron microscopy, and atomic force microscopy using magnetic signal methods to determine the complex structure and the interaction of organic compounds with magnetic Ni-Fe minerals. The presence of

Copyright © 2023 by author(s) and Scientific Research Publishing Inc. This work is licensed under the Creative Commons Attribution International License (CC BY 4.0).

<http://creativecommons.org/licenses/by/4.0/>



Open Access

Liesegang-like patterns of chondrules in fragments of the Allende structure may also be relevant to understanding how the meteorite was formed. Other observations include the presence of magnetic materials and nanorod-like solids with relatively similar sizes as well as the heterogeneous distribution of carbon in chondrules. Signals observed in the Raman and infrared spectra resemble organic compounds such as carbon nanotubes and peptide-like molecules that have been previously reported in other meteorites, making the Mexican Allende meteorite a feasible sample for the study of the early Earth and exoplanetary bodies.

Keywords

Allende Meteorite, Carbonaceous Chondrite, Light Microscopy, X-Ray Diffraction with the Rietveld Method, Raman Spectroscopy, Attenuated Total Reflectance Infrared Spectroscopy, Mass Spectrometry, Scanning Electron Microscopy, Energy Dispersive X-Ray Spectroscopy, Magnetic Force Microscopy

1. Introduction

The Allende meteorite was formed in the protoplanetary disk and may have formed at the same time as the solar system [1] [2]. This rock fell near Pueblito de Allende, a town in the southern area of the state of Chihuahua, Mexico, on February 8, 1969 [3]. The primary importance of characterizing the Allende meteorite is to understand the origins of the organic matter and minerals indigenous to the meteorite that may have been imported to Earth. The Allende meteorite is a very complex, heterogeneous rock. Several authors have disagreed on the characterization of the Allende meteorite, but several studies have shown that it contains approximately 1% metal, an average of 60% chondrules, and 40% matrix [3], and is a type III carbonaceous chondrite [4]. Various analyses of this extraterrestrial rock [5] reveal a fraction of primordial bodies that have been incorporated as pre-solar materials [6]. These studies realized that these samples could be used to understand the processes of organic molecular evolution in the universe as well as on ancient Earth. Observations of different astrophysical studies have shown that prebiotic organic synthesis took place in the solar system billions of years ago [7] [8]. At present, the most well-characterized extraterrestrial organic and mineral materials are found in meteorites [8]; they allow us to investigate the ancient co-occurrence of mineral compounds with organic matter—a cornerstone of some prebiotic experimental work [9]. The magnetic mineral content is particularly significant in the context of molecular evolution [10] [11] as they confer a shielding effect against ionizing cosmic radiation [12]. We propose that studying the mineral and organic content of the Mexican Allende meteorite can provide valuable insights into understanding the molecular evolution of the universe as well as our stellar backyard. A previous mineral analysis of Allende that gave a general description of its meteorite mineral phases was

published by Clarke *et al.* [4]. Olivine (forsterite), pyroxene (enstatite), troilite, and other mineral phases such as Ca-Al-rich aggregates and Ni-Fe magnetic alloys were among the distinctive mineral phases identified in the Allende meteorite [13]. Other studies on different meteorite classes, including the presence of magnetic minerals in ordinary and carbonaceous chondrites, have provided relevant results with wide ranges for protoplanetary disk magnetic fields, suggesting that there is a significant degree of interaction with magnetic solids at the molecular scale [14]. Based on some physicochemical considerations, it is suggested that magnetic minerals may influence the chemical activity of organic material, such as the removal of water molecules from the hydration shell in amino acids [15]. There are more than 800 different molecular compounds in carbonaceous meteorites, such as amino acids, macromolecules, and other carbon-related materials [16].

A chondrite matrix refers to the fine material that exists between chondrules, Ca-Al-rich inclusions (CAIs), as well as other inclusions or large fragments [17] that may be intimately entangled with organic compounds [18]. Carbon-containing compounds in meteorites are of scientific interest for a variety of reasons, primarily in the study of the origins of chirality in living beings [19]. Some organic compounds found in meteorites are aliphatic molecules with a wide range of molecular weights (up to 25 carbon atoms), while polycyclic aromatic hydrocarbons [20] are several orders of magnitude less concentrated in the Allende meteorite [21] [22]. Other authors have found macromolecules such as carbon nanotubes and fullerenes in the Allende meteorite [23] [24]. With a wider understanding of the molecular enrichment of the internal chondrite environment, it has been proposed that chondritic interactions that encouraged the chemical linking of amino acids, carboxylic acids, as well as both aliphatic and aromatic hydrocarbons could be related to the processes of prebiotic synthesis, similar to how glycine is related with ethanolamine [16] [20] [25] [26] [27] [28].

Previous studies have shown that Allende meteorite samples are enriched in compounds that may be related to chemical evolution [29] as well as confirmed the presence of magnetic minerals or other molecules [30]. In this study, we used improved methods for mineralogy studies to conduct a physicochemical characterization of the Allende meteorite at different scales, improving our knowledge of its integral organic and inorganic components. Our experimental results, combined with other published data, provide preliminary insights into the description of the organic compounds that occur in conjunction with magnetic minerals in the Allende meteorite. This study establishes the substantial role that these conglomerates play in the context of chemical evolution, including the addition of structural elements and compounds such as nanostructures and molecules that have not been previously reported.

2. Materials and Methods

2.1. Light Microscope Characterization of the Allende Meteorite

The meteorite is a CV3, S1, and W1 carbonaceous chondrite and was polished in

a thin sample and further analyzed using different methods. A light microscope (Motic BA310 POL, Canada) reveals chondrules of various diameters ($4.65 \mu\text{m} \pm 0.11 \mu\text{m}$).

2.2. Powder X-Ray Diffraction

X-ray Diffraction (XRD) analyses were conducted by placing the samples on a flat slab with dimensions of approximately 2.5×7.0 cm to preserve the textures and grains. Standard powder XRD patterns were recorded at room temperature in an Empyrean diffractometer with a vertical goniometer. A fixed diffracted-beam graphite monochromator (Malvern Panalytical Malvern, UK) and a PIXcel3D (Malvern Panalytical Malvern, UK) detector were used to measure the diffracted beam of X-rays produced by a $\text{CuK}\alpha$ anode (accelerating voltage of 45 kV and current of 40 mA). The 2θ range covered was from 5° to 80° , with a step size of 0.03° and a period of 40 s [31].

The Allende sample was analyzed via XRD as a complete mounted slab. An analysis of the reflections from the slab revealed the presence of ferric olivine (forsterite; $(\text{Fe}, \text{Mg})_2\text{SiO}_4$), pyroxene (diopside; $\text{CaMgSi}_2\text{O}_6$), plagioclase (albite; $\text{NaAlSi}_3\text{O}_8$), kamacite ($\text{Fe}_{0.9}\text{Ni}_{0.1}$), as well as other Ni-Fe minerals. The sample was further analyzed using the Rietveld method (background adjustment with Chebyshev function, sample displacement, phase fraction, weight fraction, microstrain, and preferred orientation employing spherical harmonic model). Rietveld refinement was improved using the GSAS-II package [32].

2.3. Raman Spectroscopy and Attenuated Total Reflection-Fourier Transform Infrared Spectroscopy (ATR-FTIR)

No additional preparation was required to acquire Raman spectra from the Allende meteorite samples. Measurements were recorded on an Optosky ATR3000 portable Raman spectrometer (Software Park, Jimei, Xiamen, China) with an ultra-high sensitivity CCD detector (785 nm exciting laser with an operating depth of 3.0 mm into the sample and a spectral range of $200 - 3500 \text{ cm}^{-1}$). The power of the laser was set to 400 mW and 0.6 match.

The infrared spectra were obtained with an ATR-FTIR instrument (Spectrum 100 FT-IR Spectrometer Perkin Elmer, Waltham, Massachusetts, USA) between $4000 - 650 \text{ cm}^{-1}$ (6 scans). The ATR-FTIR was first performed on the ground sample, acquiring data that revealed the bands typical for the Allende meteorite. A powdered sample was used to avoid the signals introduced due to the environmentally exposed nature of the sample. A second inspection consisted of an analysis of the second derivative of the signal using the Spectrum software (PerkinElmer), version 6.2.0.

2.4. Mass Spectrometry-Electrospray Ionization-High-Performance Liquid Chromatography

The core and crust of the Allende meteorite were analyzed using this procedure.

The powdered samples of the Allende meteorite as well as basalt from the Popocatepetl volcano (from the Cacaxtla/Xochitécatl Archaeological Site) were placed in cellulose cartridges and inserted into a Soxhlet Extraction Apparatus. The basalt from Popocatepetl volcano was used to detect the different molecular masses that may have been introduced due to the weathering of the Allende meteorite. A mix of acetone-methanol (60% - 40% v/v) was used as a solvent. The extracted residues were analyzed by the mass spectrometer instrument due to their high sensitivity with regard to the detection of different organic molecules at very low concentrations. An HPLC system (515 HPLC pump, Waters Corp.), a single quadrupole mass detection system (SQ-2 Waters Corp.), and an electronic distance measurement instrument (EDM) in negative mode (ESI-) were used. The settings used for the instrument were as follows: 1.95 kV capillary, 39 V at a temperature of 350°C, and a desolvation gas flow of 650 L/h using a direct infusion system.

2.5. Scanning Electron Microscopy and Elemental Analysis

The morphological and elemental characterization of the Allende meteorite was conducted using Scanning Electron Microscopy (SEM) and Energy-Dispersive X-ray spectroscopy (EDS) in a Zeiss EVO10 instrument/Bruker XFlash 6 - 30 detector (15.0 kV). The SEM image was acquired with the backscattering detector placed at a working distance of 11.3 mm.

2.6. Atomic and Magnetic Force Microscopy Characterization

A more detailed analysis of the structures on the polished surface of the Allende meteorite and their physical properties were performed using a JEOL JSPM-5200 (Akishima, Tokyo, Japan) scanning probe microscope in tapping mode. A probe with a nominal resonance frequency of 300 kHz and a constant force of 40 N/m was used for topographic analysis. A probe with a frequency of 75 kHz and a constant force of 3 N/m was used to evaluate the sample's magnetic properties. The gradients of the magnetic force were acquired with a magnetic CoCr-coated tip exposed to a static magnetic field of approximately 5000 Gauss.

3. Results

3.1. Matrix Morphology

The Allende meteorite is relevant to studies on meteoritic composition, and can significantly increase our knowledge of the solar system due to its mineral content, texture, and magnetic properties [33]. Allende is a CV3 chondrite with a granular structure that is visible under a light microscope (**Figure 1**). The Allende chondrite consists of chondrules, CAIs, and opaque minerals (iron-nickel alloys, troilite, and magnetite) surrounded by a fine-grained black matrix. Chondrules can be clearly identified under transmitted light and appear to be aligned (**Figure 1(A)**). The various shapes and textures of the Allende indicate a complex structure that resembles the Liesegang rings (to wide the eye see the yellow

lines in **Figure 1(B)**; (Liesegang 1907)). **Figure 1(A)** highlights the presence of the semi-circular ring-like ordered chondrules that are possibly formed by accretion named by us as Liesegang-like rings. **Figure 1(B)** highlights the semi-circular distribution of the chondrules. The semi-circular lines appear to be sedimentary ring-like patterns (**Figure 1(B)**). **Figure 1(C)** shows the matrix (black regions) and chondrules of various sizes (the transparent areas), while **Figure 1(D)** shows the solid areas inside the chondrules.

3.2. X-Ray Diffraction

The crystalline phases were identified by extracting structural information from the XRD spectra, revealing the presence of ferric olivine ($(\text{Fe}, \text{Mg})_2\text{SiO}_4$), diopside ($\text{CaMgSi}_2\text{O}_8$), albite ($\text{NaAlSi}_3\text{O}_8$), and kamacite ($\text{Fe}_{0+0.9}\text{Ni}_{0.1}$). In addition, other Ni-Fe minerals may be present. Rietveld refinement was carried out using the GSAS-II software package [32].

Due to the weight fraction of the kamacite and other Ni-Fe phases (such as whewellite) in the preliminary Rietveld analysis (less than 1%), these minerals are considered to be rare. The weight fraction of each refined phase was 68.3% ferric olivine, 18.5% diopside, and 13.1% albite (**Figure 2**).

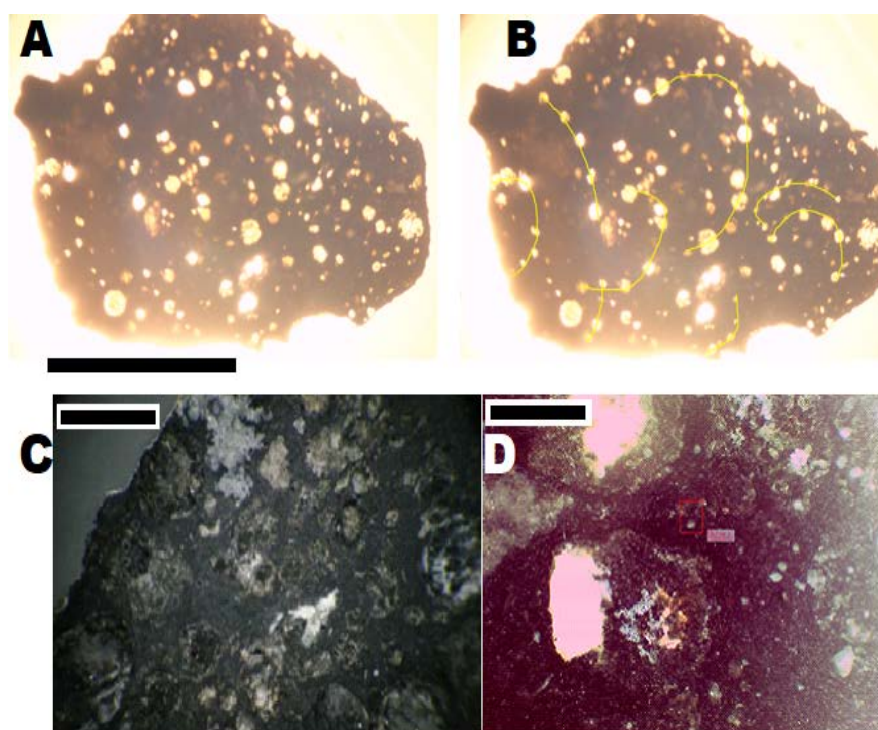


Figure 1. The Allende meteorite is a CV3 chondrite with a granular structure visible under light microscopy. (A) Chondrules are arranged in ring-like order, suggesting a formation by accretion. In this work the proposed name is Liesegang-like rings. (B) The yellow lines show the semi-circular distribution of chondrules that has a diagenetic ring-like appearance (scale bar ≈ 2.0 cm). (C) The matrix (black regions) and chondrules (the transparent regions) (scale bar ≈ 500 μm). (D) A closeup of the chondrules (scale bar ≈ 100 μm).

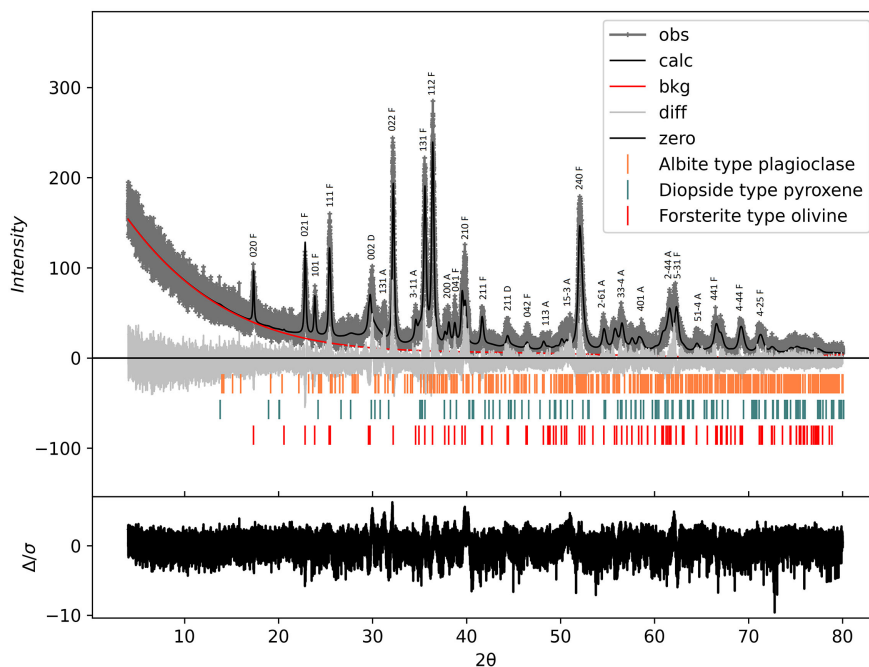


Figure 2. The structural characterization performed on the Allende meteorite by X-ray diffraction presented the characteristic crystallographic planes of the albite, diopside, and forsterite olivine minerals (A, D and F in the peaks correspondingly). The XRD spectra as well as Rietveld refinement conducted on the Allende meteorite are shown. For this procedure, a complete, polished slab was used to maintain the texture of the mineral phases. The primary minerals (albite, diopside, and olivine) observed correspond to the gray line, while the solid black line refers to the calculated minerals. Minor mineral phases were adjusted to the kamacite reflections. The differences are represented in the zero-line plots; each corresponds to Bragg reflections in crystalline phases. The black plot at the bottom describes the difference between the observed and calculated diffractograms.

3.3. Raman and Infrared Spectroscopy

The Raman spectra of the Allende meteorite revealed the presence of numerous components in the matrix and chondrules, suggesting the possible presence of carbon nanostructures (**Figure 3(A)**). The identified signals correspond to nano-diamonds ($\sim 1326, 1600 \text{ cm}^{-1}$), glass ($\sim 580, 790, 1100$ and 1900 cm^{-1}) [34], nanotubes ($\sim 1625 \text{ cm}^{-1}$) [35], and minerals such as kamacite (<https://rruff.info/Kamacite>) and olivine ($1800 - 1900 \text{ cm}^{-1}$) [36]. Sulfides, in the form of troilite, exhibit active weak modes at 290 and 335 cm^{-1} [37]. The ATR-FTIR spectra of the Allende meteorite were obtained directly from the ground material (**Figures 3(B)-(E)**). Second derivative ATR-FTIR spectra were obtained after inspection of the FTIR bands (**Figure 3(B)** and **Figure 3(D)**) to increase the sensitivity of the bands. The Allende samples were collected on location, and thus differential signals were expected due to the organic compounds from the natural environment. In other words, the Raman and FTIR signals reflect the contributions of both terrestrial and extraterrestrial carbon-related compounds. Possible amide II ($\sim 1550 \text{ cm}^{-1}$) and amide I ($\sim 1650 \text{ cm}^{-1}$) signals from peptides (vertical bars) as well as other C=O, C=C, and C=N signals in the region between $1800 - 1500 \text{ cm}^{-1}$ were

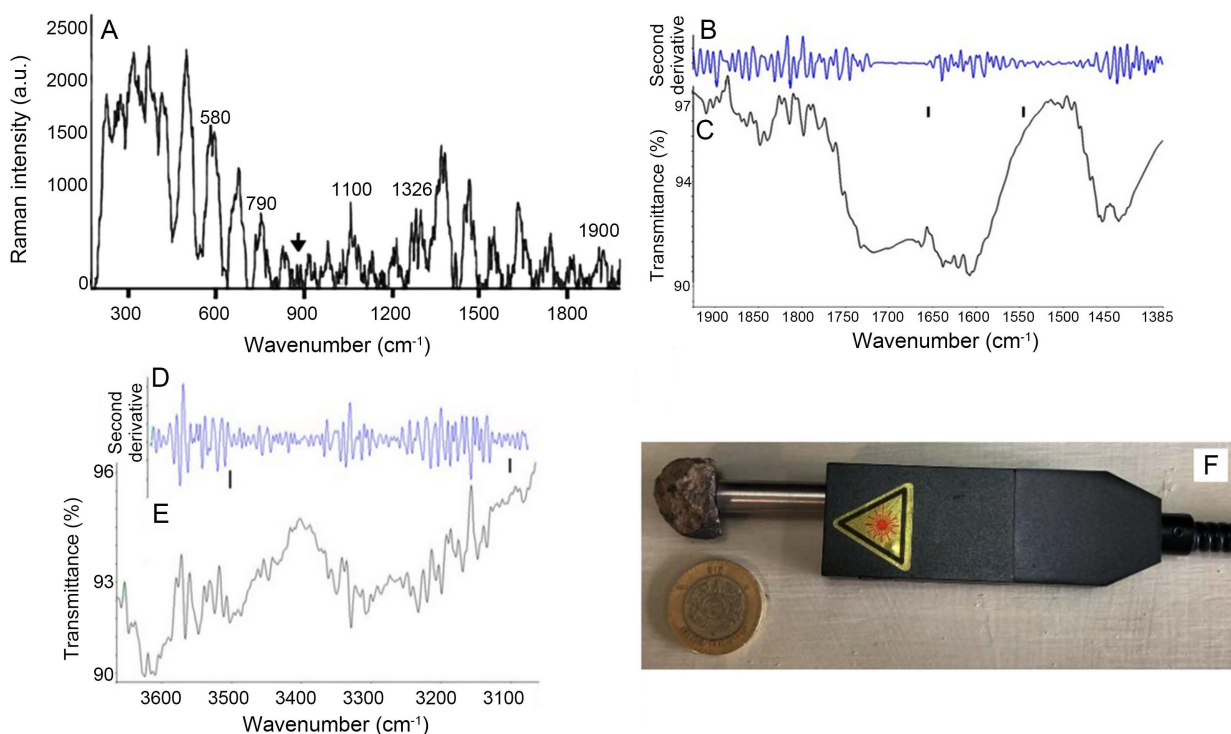


Figure 3. (A) Raman spectra of the Allende meteorite showcasing the possible presence of nanodiamond signals (~ 1326 , 1600 cm^{-1}), glass bands (~ 580 , 790 , 1100 , and 1900 cm^{-1}), possible nanotubes ($\sim 1625\text{ cm}^{-1}$; black arrow), and other minerals such as kamacite ($\sim 300\text{ cm}^{-1}$). (B) The second derivative of the bands in the region between 1900 and 1450 cm^{-1} highlights the presence of possible small amide II (ca. 1550 cm^{-1}) and amide I (ca. 1650 cm^{-1}) signals that are characteristic of peptides (vertical bars). (D) The FTIR spectra of the Allende meteorite, with the (E) second derivative suggesting the presence of A (3500 cm^{-1}) and B (3100 cm^{-1}) amide bands (vertical bars in D) in the 3600 cm^{-1} to 3100 cm^{-1} region. (F) Raman spectra were collected from whole Allende samples using an ATR portable Raman spectrometer (coin diameter ca. 3.0 cm).

identified. In the FTIR spectra, the $3600 - 3100\text{ cm}^{-1}$ region contained the A (3500 cm^{-1}) and B (3100 cm^{-1}) amide bands (vertical bars in **Figure 3(D)**).

3.4. Mass Spectrometry-Electrospray Ionization-High-Performance Liquid Chromatography

In the mass spectra presented in **Figure 4**, different masses correspond to the signals in the analyzed samples. Total ion current peaks at 60 and 90 m/z correspond to the solvent used in the extraction process. The basalt from the Popocatepetl volcano has a signal that is very similar to the core and crust of the Allende meteorite (**Figure 4**). These signals correspond to high molecular weight organic matter (e.g., 230 and 244 m/z). A more detailed inspection of the **Figure 4(C)** shows (black arrows) some masses possibly characteristic of the core sample (ca. 127 m/z and ca. 195 m/z). The characterization of these masses must be a subject of more accurate analysis and thus confirm the mass differences by means of an analysis of higher resolution.

3.5. Scanning Electron Microscopy

The diversity of the micro-structures observed by optical microscopy was analyzed in greater detail by SEM (**Figure 5**). In the backscattered electron (BSE)

micrographs, a wide diversity of structures (**Figure 5** and **Figure 6(A)**) and chemical compositions (**Figures 6(B)-(K)**) was observed.

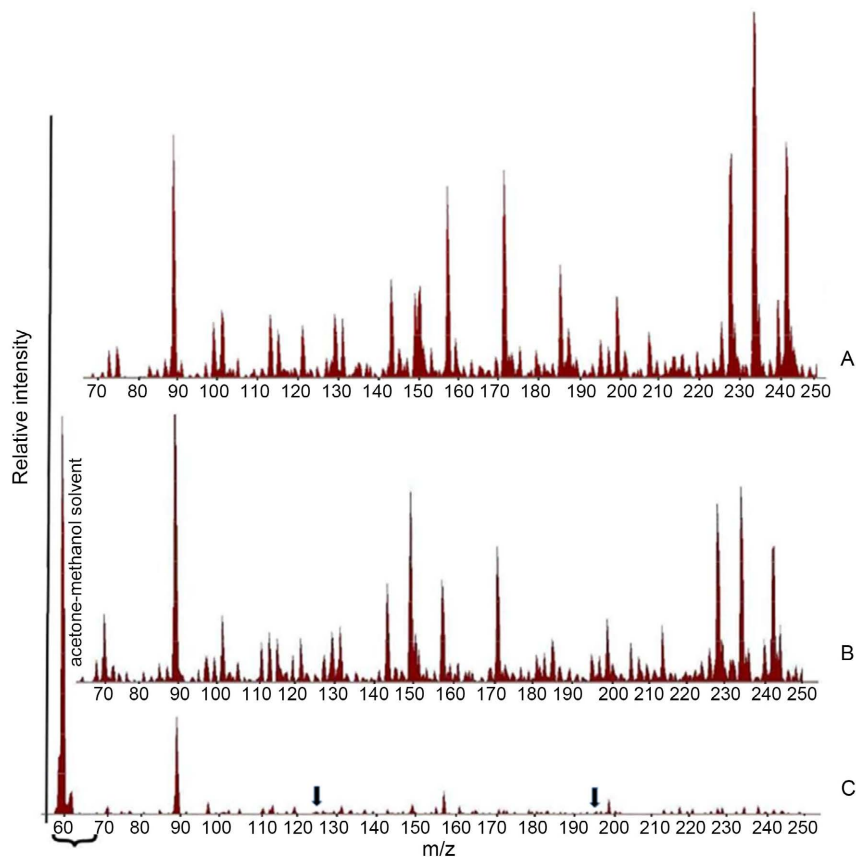


Figure 4. Comparison of the mass spectra from extracted samples of (A) the core of the Popocatepetl basalt volcano rock (obtained from the Cacaxtla/Xochitcatl Archaeological Site), (B) the outer layer of the Allende meteorite, and (C) the core section of the Allende meteorite. The square brackets indicate the peaks that correspond to the acetone-methanol solvent (60%/40% v/v).

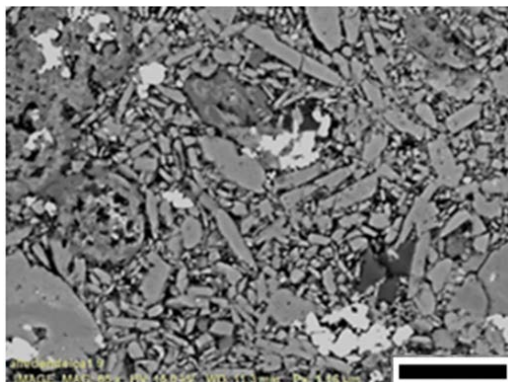


Figure 5. The BSE micrograph of the Allende meteorite CV3 matrix reveals the diverse structures and compositions due to differences in the dispersion factor of the atoms that conform to each zone, as indicated by the gray contrast (scale bar 200 nm).

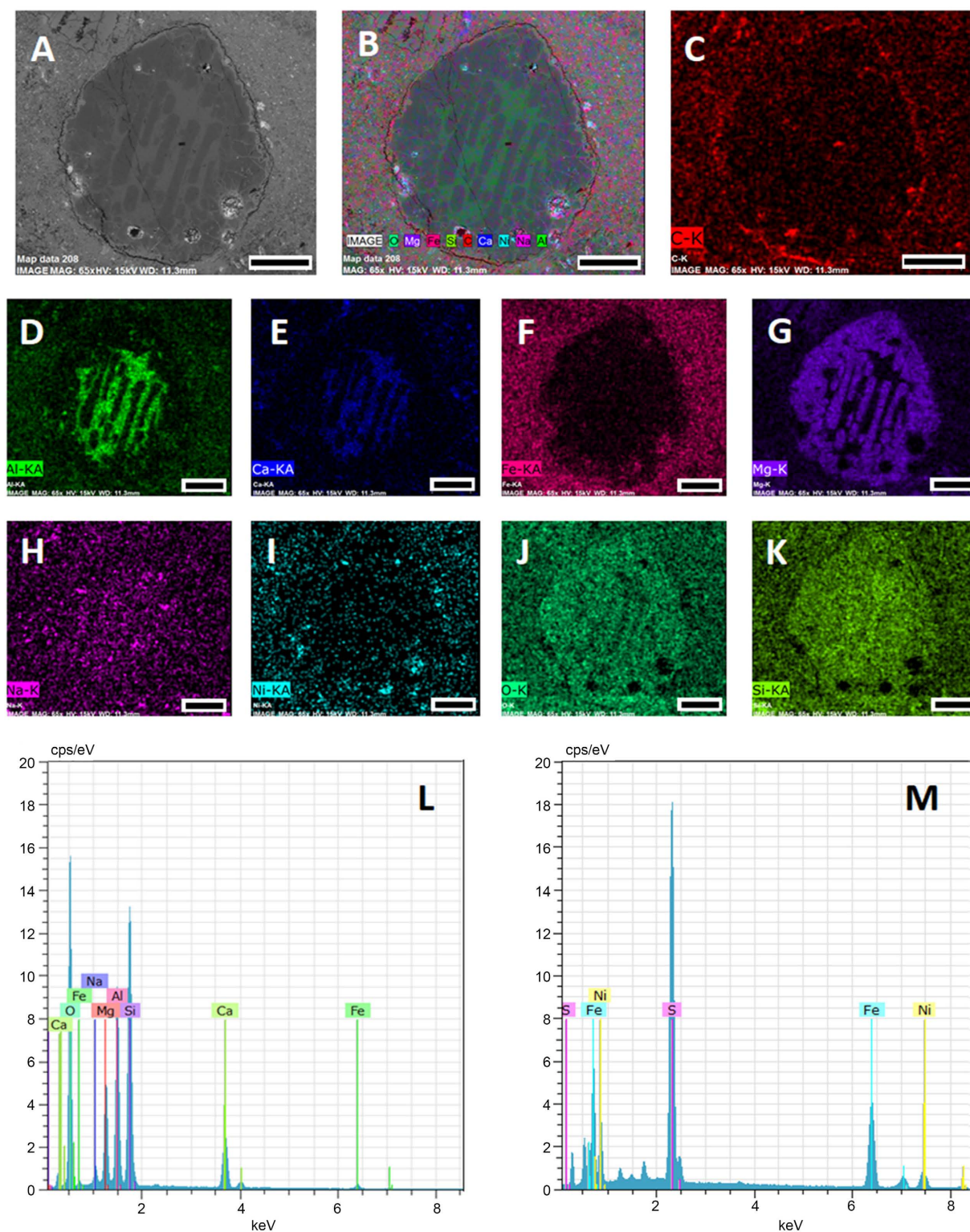


Figure 6. The BSE micrographs of the Allende meteorite obtained by SEM showcase the different distributions of Al, Ca, Fe, Mg, Na, Ni, O, and Si in the barred chondrules in the sample. In these micrographs, lighter colors indicate a higher concentration of elements. The EDS analysis maps the structural features to the chemical composition using a false color composite (B)-(K). There is a clear contrast in the colors in some areas of (B) and (C), which corresponds to the distribution of carbon. In addition to these analyzed areas, the EDS signals indicate similar elemental content in chondrules (L) and matrix (M) with a difference in presence of sulfur and nickel in the matrix (M). Scale bars = 200 μm .

The elemental chemical composition of the samples was obtained using EDS. The results were subsequently correlated with the phases identified in the XRD spectra to obtain the electron microscope images (**Figure 6**).

The BSE micrographs were taken from multiple areas across the sample show that there are great differences between zones (**Figure 5** and **Figure 6**), indicating that there is a significant variation in chemical composition. For instance, the local heterogeneous distribution of carbon suggests that these differences are due to the native elemental matter of the meteorite (**Figure 6(C)**).

EDS analyses were performed on chondrules and matrix zones of the Allende meteorite (**Figure 6**). In general, the elemental analysis in the chondrule matrix showed that it consisted of oxygen (60%), silicon (16.5%), aluminum (~10%), magnesium (~6.0%), iron (~1.0%), and sodium (~1.0%), with an accuracy of 1 sigma of the atomic content (%). Inside the barred structures, the most abundant elements were oxygen (~56.8%), magnesium (~28.2%), silicon (~14%), iron (0.8%), and calcium (0.42%). In contrast, the elemental content of the matrix was oxygen (57.4%), iron (13%), silicon (12%), magnesium (12.3%), aluminum (2.0%), calcium (0.98%), sulfur (1.1%), nickel (0.56%), and sodium (0.68%). The Allende structures are characterized by variable compositions [33] [34] [35]. The elemental analysis is consistent with the XRD spectra, with a composition composed of kamacite ($\text{Fe}_{0+0.9}$, $\text{Ni}_{0.1}$), pyroxene ($\text{CaMgSi}_2\text{O}_8$), olivine ($(\text{Fe}, \text{Mg})_2\text{SiO}_4$), and possibly glass (the background in **Figure 2**).

In the matrix of the Allende CV3 chondrite the ferrous olivine with a Fe_{30-60} composition (fayalite) is among the main mineral content. In contrast, the olivine in chondrules is more forsteritic in nature, possessing more Mg than Fe (**Figure 6(F)** and **Figure 6(G)**). It also contains sulfide, some iron-nickel alloy grains, troilite, sodalite, Ca-rich pyroxene ($\text{En}_{48}\text{Wo}_{43}$), and magnetite. The glassy mesostasis between olivine bars is feldspathic as shown by **Figure 6(D)**, **Figure 6(E)**, and **Figure 6(H)**. The chondrules are surrounded by carbon-rich compounds (**Figure 6(C)**).

3.6. Atomic and Magnetic Force Microscopy

Atomic force microscope (AFM) images were used to provide further insights into the complex organization of the samples (**Figure 7**). A petrographic thin section was used for this purpose (**Figure 1(A)**); no further chemical preparation was required (**Figure 6**).

Compared with the light microscopy and SEM images, the AFM images allowed for the magnification of the topographical and structural data of the samples. AFM permitted the exploration of the polished surface through the topography, phase, and magnetic images at the nanometer scale (**Figure 7(B)** and **Figure 7(C)**). The varying size and composition of the chondrules make characterization difficult using other microscopy methods; a more detailed analysis is possible using AFM data. The AFM analysis revealed the presence of some mineral structures, but no carbon-related nanostructures were observed. However, indirect structural evidence suggests the presence of silicate minerals (**Figure 7**).

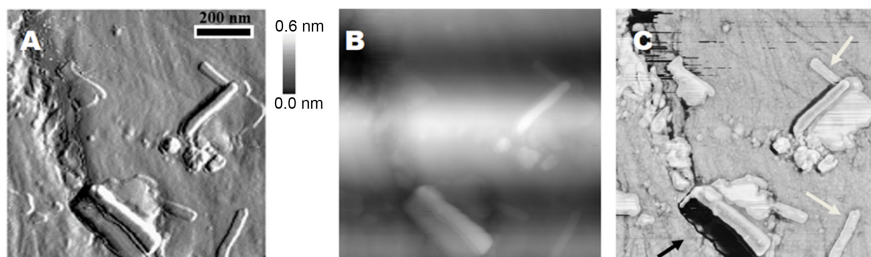


Figure 7. AFM topography (A) and phase (B) images that show the nanoscale structures in the Allende meteorite (scale bar is the same for the three AFM images). The height contours in (A) highlight the homogeneity of the flat surface observed in the thin section. (C) The magnetic signal highlights two nanoscale magnetic domains (black arrow) as well as unidentified nanorods (white arrows).

The planarity of the surface of the Allende samples helped to identify such structures and allowed us to acquire magnetic images with no interference from the topography (Figure 7).

AFM was also used to measure the local magnetic (MFM) properties (Figure 7(C)), revealing the presence of nanoscale magnetic domains (black arrow). The nanorods embedded in the matrix (white arrows; Figure 7(C)) had similar dimensions; they were ~5 nm in diameter and ~250 nm in length. The homogeneity in the dimensions of the rods is consistent with structures described as nanotubes in other studies [38] [39], although only nanorods were observed in these samples. In addition, the magnetic response in Figure 7(C) may be attributed to the presence of multiple magnetic materials, such as the kamacite identified using the Rietveld refinement (Figure 2). Magnetic force microscopy also shows the attractive (black arrow; Figure 7(C)) and repulsive magnetic forces (Figure 7(C)). These AFM features do not provide enough information to identify the mineralogy. The AFM images show well-fixed structures instead of mobile ones, indicating that the matrix is dense and well-consolidated; no additional patterns were observed in the phase image (Figure 7(B)), which highlights the homogeneous, compact nature of the structure. Furthermore, the lines were created during the preparation of the thin, diamond-cut section in the three images (Figure 7). These results imply that the observed structures are consolidated solids in the matrix of the Allende meteorite.

4. Discussion

The analysis of the Allende meteorite presented in this work indicates the presence of Liesegang-like growths composed of chondrules (Figure 1(A) and Figure 1(B)) [40]. Previous studies have attempted to describe the patterning and meteoritic structures in the Allende samples [41]. This study reports on clear patterns observed in the samples. The novel precipitation process described here paves the way for an understanding of the formation and consolidation of the original rock. The described heterogeneous structure of the meteorite reflects the complex environmental conditions during its formation. The chondrules display

circular patterns at higher magnifications (**Figure 1(C)** and **Figure 1(D)**) that are dominated by dark regions and white particles comprised of olivine, pyroxene, and albite (**Figure 1**); this is consistent with previous studies [42]. Rietveld refinement revealed a presence of other previously reported minerals in the Allende meteorite, such as kamacite and possibly whewellite. The presence of kamacite was confirmed by XRD and Raman spectra ($\sim 300\text{ cm}^{-1}$); kamacite is also known to appear in iron meteorites [43]. The local Ni-Fe enrichment of the Allende meteorite provides insights into the diversity of Ni-Fe-based compounds in carbonaceous chondrites. The diversity of the minerals observed in this study and confirmed in other analysis [44] indicates that these compounds may be present in early scenarios of the solar system and in the formation of our planet. In our study, carbon-related compounds are only detected by Raman spectra (**Figure 3(A)**), FTIR (**Figures 3(B)-(E)**), and mass spectroscopy (**Figure 4**). The Raman spectra exhibit a shift that may indicate possible nanostructures (nanodiamond signals at $\sim 1326, 1600\text{ cm}^{-1}$), glass (ca. $580, 790, 1100, \text{ and } 1900\text{ cm}^{-1}$), nanotubes ($\sim 1625\text{ cm}^{-1}$ black arrow), as well as other minerals. The FTIR spectra suggest the presence of amide II ($\sim 1550\text{ cm}^{-1}$) and amide I ($\sim 1650\text{ cm}^{-1}$) signals that are characteristic of peptides, although the presence of these bands cannot be used to determine their chemical origins or the nature of the molecules. Similarly, the precise nature of the mass spectra and their chemical origins are still unknown (**Figure 4**). For example, similar signals are observed in the mass spectra of both the Popocatepetl (Cacaxtla/Xochit catl) basalt sample and the Allende sample, making it difficult to determine which fractions of the Allende meteorite were formed on Earth and which were a modification of the indigenous material. In other words, to improve this analysis, additional studies must be conducted to gain insight into the molecular origin of the possible peptide signals as well as the materials identified in the mass spectra such as the ca. 127 m/z and ca. 195 m/z . This study also shows that terrestrial organics may have contaminated the Allende meteorite, as evidenced by the mass spectroscopy similarities between the crust of the Allende meteorite and Xochit catl/Popocatepetl sample (**Figure 4**), the SEM images obtained from Allende's complex structure (**Figures 4-6**), and the elemental analysis (**Figures 6(D)-(M)**). Future analysis may wish to acquire mass spectra from the core of the Allende meteorite to determine if the indigenous masses from this region of the meteorite are different from the Xochit catl/Popocatepetl basalt rock and the crust of the Allende meteorite. Furthermore, the variations in the carbon abundance may be dependent on the elemental distribution in the meteorite (**Figure 6(C)**). The increased abundance of carbon detected around the chondrules represents a potential site where prebiotic chemistry and molecular evolution can take place. However, it is not possible to suggest the mechanism for the distribution of elements—in particular, carbon—based on these data. Additionally, although the nanoscale carbon-related solids in the AFM images (**Figure 7(A)** and **Figure 7(B)**) are not correlated with the SEM topography, these images confirm the structural con-

densation of portions of the Allende meteorite, which contain magnetic solids and their interaction with carbon-related compounds. In addition, we wish to highlight the analysis and exploration conducted by the atomic and magnetic force microscope methodology. It is possible to recognize nanorods and other particles; future work should investigate these structures in more detail. Even with this limited analysis, the Allende meteorite represents the interaction of different materials and physicochemical conditions and highlights several specific processes that lead to the formation of meteoritic structures.

5. Conclusions

The characterization of the Allende meteorite in this work reveals Liesegang-like growth patterns composed of chondrules. This complex, heterogeneous structure may reflect the environmental conditions that were present during the formation of this rock. Furthermore, the distribution of carbon-related compounds, although not clear, reflects the heterogeneous origins of the Allende meteorite; this is substantiated by the different spectra collected in this study. Raman and FTIR spectroscopy suggest the existence of these carbon-related signals, such as the presence of amide II and I bands from proteinaceous organic compounds whereas the mass spectrometry data collected here will be used to spatially resolve the distribution of the organic, terrestrial and extraterrestrial, compounds.

However, these data were not sufficient to suggest a mechanism for the distribution and origin of the elements within the meteorite, especially in the context of organic compounds. The contribution of carbon to the nanostructures, nanodiamonds, and possibly amino acids could also not be determined. The experimental work presented reported that the data obtained from the direct analysis of the agglomeration structures in these meteorites may provide information about prebiotic chemistry and the formation of the protoplanetary disk. The heterogeneous distribution of chondrules, which form rings or Liesegang-like rings, the diversity of elemental content and its distribution in chondrules in association with magnetic minerals, and the nanostructures presented here serve to complement the structural and magnetic characterization of the Allende meteorite. Future work will focus on the characterization of the magnetic properties of the Allende as well as their possible relevance to the reactivity of organic molecules in the context of oligomer formation, structural selectivity, and chemical stability. Similarly, we intend to expand the experimental work to include an analysis of the mass spectrometry data as well as computer simulations for the physicochemical molecular reactions associated with the molecular structure and molecular evolution of the meteorites. The inorganic prebiotic conditions in the Allende meteorite are of main relevance as to be considered in our future studies to understand their role on the molecular evolution towards more complex physicochemical systems.

Funding

This research was funded by DGAPA PAPIIT Project IN205522.

Acknowledgements

We would like to thank Dr. Margarita Reyes Salas (SEM analysis) and Dr. Teresa Pi Puig from Departamento de Procesos Litosféricos, Instituto de Geología, Universidad Nacional Autónoma de México, and Laboratorio Nacional de Geoquímica y Mineralogía LANGEM for all of their work as well as Angeles Martínez Gómez (angeles.ironika@gmail.com) for the design. We would like to thank BSc Claudia Consuelo Camargo Raya, M. in Sc. Paola Molina Sevilla (Departamento de Química de Radiaciones y Radioquímica, ICN, UNAM), Mr. Rangel Gutiérrez, Mr. Valle Almazán (ICN, UNAM) and M. in Educ. Isabel Mejía Luna (Departamento de Física, Carrera de Ciencias de la Tierra, Facultad de Ciencias, UNAM and Escuela Nacional de Ciencias de la Tierra, UNAM). We would like to also thank Luciano Díaz González, Martín Cruz Villafañe, Luis Miguel Valdez Pérez, Ing. Juan Eduardo Murrieta León, Mat. Enrique Palacios Boneta and Phys. Antonio Ramírez Fernández for their technical assistance.

Conflicts of Interest

The authors declare no conflicts of interest regarding the publication of this paper.

References

- [1] Brenker, F.E., Palme, H. and Klerner, S. (2000) Evidence for Solar Nebula Signatures in the Matrix of the Allende Meteorite. *Earth and Planetary Science Letters*, **178**, 185-194. [https://doi.org/10.1016/S0012-821X\(00\)00075-3](https://doi.org/10.1016/S0012-821X(00)00075-3)
- [2] McCoy, T.J. and Corrigan, C.M. (2021) The Allende Meteorite: Landmark and Cautionary Tale. *Meteoritics & Planetary Science*, **56**, 5-7. <https://doi.org/10.1111/maps.13613>
- [3] King, E.A., Schonfeld, E., Richardson, K.A. and Eldridge, J.S. (1969) Meteorite Fall at Pueblito de Allende, Chihuahua, Mexico: Preliminary Information. *Science*, **163**, 928-929. <https://doi.org/10.1126/science.163.3870.928>
- [4] Clarke, C., Roy S., Jarosewich, E., Mason, B., Nelen, J., Gomez, M. and Hyde, J.R. (1971) Allende, Mexico, Meteorite Shower. *Smithsonian Contributions to the Earth Sciences*, 1-53. <https://doi.org/10.5479/si.00810274.5.1>
- [5] Jarosewich, E., Clarke, C., Roy S. and Barrows, J.N. (1987) Allende Meteorite Reference Sample. *Smithsonian Contributions to the Earth Sciences*, 1-49. <https://doi.org/10.5479/si.00810274.27.1>
- [6] del Sol Hernández-Bernal, M. and Solé, J. (2010) Single Chondrule K-Ar and Pb-Pb Ages of Mexican Ordinary Chondrites as Tracers of Extended Impact Events. *Revista mexicana de ciencias geológicas*, **27**, 123-133.
- [7] Kwok, S. (2016) Complex Organics in Space from Solar System to Distant Galaxies. *The Astronomy and Astrophysics Review*, **24**, Article No. 8. <https://doi.org/10.1007/s00159-016-0093-y>
- [8] Irvine, W.M. (1998) Extraterrestrial Organic Matter: A Review. *Origins of Life and Evolution of the Biosphere*, **28**, 365-383. <https://doi.org/10.1023/A:1006574110907>
- [9] Cleaves, H. (2013) Prebiotic Chemistry: Geochemical Context and Reaction Screening. *Life*, **3**, 331-345. <https://doi.org/10.3390/life3020331>

- [10] Angeles-Camacho, E., Cruz-Castañeda, J., Meléndez, A., Colín-García, M., de la Cruz, K.C., Ramos-Bernal, S., Negrón-Mendoza, A., Garza-Ramos, G., Rodríguez-Zamora, P., Camargo-Raya, C., *et al.* (2020) Potential Prebiotic Relevance of Glycine Single Crystals Enclosing Fluid Inclusions: An Experimental and Computer Simulation with Static Magnetic Fields. *Advances in Biological Chemistry*, **10**, 140-156. <https://doi.org/10.4236/abc.2020.105011>
- [11] Heredia, A., Colín-García, M., Puig, T.P.I., Alba-Aldave, L., Meléndez, A., Cruz-Castañeda, J.A., Basiuk, V.A., Ramos-Bernal, S. and Mendoza, A.N. (2017) Computer Simulation and Experimental Self-Assembly of Irradiated Glycine Amino Acid under Magnetic Fields: Its Possible Significance in Prebiotic Chemistry. *Biosystems*, **162**, 66-74. <https://doi.org/10.1016/j.biosystems.2017.08.008>
- [12] Nakashima, S., Kebukawa, Y., Kitadai, N., Igisu, M. and Matsuoka, N. (2018) Geochemistry and the Origin of Life: From Extraterrestrial Processes, Chemical Evolution on Earth, Fossilized Life's Records, to Natures of the Extant Life. *Life*, **8**, Article 39. <https://doi.org/10.3390/life8040039>
- [13] Kletetschka, G. (2018) Magnetization of Extraterrestrial Allende Material May Relate to Terrestrial Descend. *Earth and Planetary Science Letters*, **487**, 1-8. <https://doi.org/10.1016/j.epsl.2018.01.020>
- [14] Urrutia-Fucugauchi, J., Pérez-Cruz, L. and Flores-Gutiérrez, D. (2014) Meteorite Paleomagnetism—From Magnetic Domains to Planetary Fields and Core Dynamoes. *Geofísica Internacional*, **53**, 343-363. [https://doi.org/10.1016/S0016-7169\(14\)71510-7](https://doi.org/10.1016/S0016-7169(14)71510-7)
- [15] De Ninno, A. and Congiu Castellano, A. (2014) Influence of Magnetic Fields on the Hydration Process of Amino Acids: Vibrational Spectroscopy Study of L-Phenylalanine and L-Glutamine. *Bioelectromagnetics*, **35**, 129-135. <https://doi.org/10.1002/bem.21823>
- [16] McGeoch, J.E.M. and McGeoch, M.W. (2015) Polymer Amide in the Allende and Murchison Meteorites. *Meteoritics & Planetary Science*, **50**, 1971-1983. <https://doi.org/10.1111/maps.12558>
- [17] Simon, J.I., Cuzzi, J.N., McCain, K.A., Cato, M.J., Christoffersen, P.A., Fisher, K.R., Srinivasan, P., Tait, A.W., Olson, D.M. and Scargle, J.D. (2018) Particle Size Distributions in Chondritic Meteorites: Evidence for Pre-Planetesimal Histories. *Earth and Planetary Science Letters*, **494**, 69-82. <https://doi.org/10.1016/j.epsl.2018.04.021>
- [18] Pizzarello, S., Schrader, D.L., Monroe, A.A. and Lauretta, D.S. (2012) Large Enantiomeric Excesses in Primitive Meteorites and the Diverse Effects of Water in Cosmochemical Evolution. *Proceedings of the National Academy of Sciences of the United States of America*, **109**, 11949-11954. <https://doi.org/10.1073/pnas.1204865109>
- [19] Sephton, M.A. (2005) Organic Matter in Carbonaceous Meteorites: Past, Present and Future Research. *Philosophical Transactions of the Royal Society A: Mathematical, Physical and Engineering Sciences*, **363**, 2729-2742. <https://doi.org/10.1098/rsta.2005.1670>
- [20] Zenobi, R., Philippoz, J.M., Buseck, P.R. and Zare, R.N. (1989) Spatially Resolved Organic Analysis of the Allende Meteorite. *Science*, **246**, 1026-1029. <https://doi.org/10.1126/science.246.4933.1026>
- [21] Levy, R.L., Wolf, C.J., Grayson, M.A., Gilbert, J., Gelpi, E., Updegrove, W.S., Zlatkis, A. and Oro, J. (1970) Organic Analysis of the Pueblito de Allende Meteorite. *Nature*, **227**, 148-150. <https://doi.org/10.1038/227148a0>
- [22] Han, J., Simoneit, B.R., Burlingame, A.L. and Calvin, M. (1969) Organic Analysis on

- the Pueblito de Allende Meteorite. *Nature*, **222**, 364-365.
<https://doi.org/10.1038/222364a0>
- [23] Cruz-Rosas, H.I., Riquelme, F., Santiago, P., Rendón, L., Buhse, T., Ortega-Gutiérrez, F., Borja-Urby, R., Mendoza, D., Gaona, C., Miramontes, P., *et al.* (2019) Multiwall and Bamboo-like Carbon Nanotubes from the Allende Chondrite: A Probable Source of Asymmetry. *PLOS ONE*, **14**, e0218750.
<https://doi.org/10.1371/journal.pone.0218750>
- [24] Harris, P.J.F., Vis, R.D. and Heymann, D. (2000) Fullerene-Like Carbon Nanostructures in the Allende Meteorite. *Earth and Planetary Science Letters*, **183**, 355-359.
[https://doi.org/10.1016/S0012-821X\(00\)00277-6](https://doi.org/10.1016/S0012-821X(00)00277-6)
- [25] Hare, P.E., Hoering, T.C. and King, K. (1980) Biogeochemistry of Amino Acids. Warrenton, Virginia, October 29-November 1 1978, Wiley, New York.
- [26] McGeoch, J.E.M. and McGeoch, M.W. (2014) Polymer Amide as an Early Topology. *PLOS ONE*, **9**, e103036. <https://doi.org/10.1371/journal.pone.0103036>
- [27] McGeoch, J.E.M. and McGeoch, M.W. (2017) A 4641Da Polymer of Amino Acids in Acfer 086 and Allende Meteorites. arXiv: 1707.09080.
- [28] Zhang, X., Tian, G., Gao, J., Han, M., Su, R., Wang, Y. and Feng, S. (2017) Prebiotic Synthesis of Glycine from Ethanolamine in Simulated Archean Alkaline Hydrothermal Vents. *Origins of Life and Evolution of Biospheres*, **47**, 413-425.
<https://doi.org/10.1007/s11084-016-9520-3>
- [29] Lo, Y.H., Liao, C.T., Zhou, J., Rana, A., Bevis, C.S., Gui, G., Enders, B., Cannon, K.M., Yu, Y.S., Celestre, R., *et al.* (2019) Multimodal X-Ray and Electron Microscopy of the Allende Meteorite. *Science Advances*, **5**, eaax3009.
<https://doi.org/10.1126/sciadv.aax3009>
- [30] Fisun, O.I. and Savin, A.V. (1992) Homochirality and Long-Range Transfer in Biological Systems. *Biosystems*, **27**, 129-135.
[https://doi.org/10.1016/0303-2647\(92\)90068-A](https://doi.org/10.1016/0303-2647(92)90068-A)
- [31] Morales-Pérez, A., Moreno-Rodríguez, V., Del Rio-Salas, R., Imam, N.G., González-Méndez, B., Pi-Puig, T., Molina-Freaner, F. and Loredó-Portales, R. (2021) Geochemical Changes of Mn in Contaminated Agricultural Soils Nearby Historical Mine Tailings: Insights from XAS, XRD and, SEP. *Chemical Geology*, **573**, Article ID: 120217. <https://doi.org/10.1016/j.chemgeo.2021.120217>
- [32] Toby, B.H. and Von Dreele, R.B. (2013) GSAS-II: The Genesis of a Modern Open-Source All Purpose Crystallography Software Package. *Journal of Applied Crystallography*, **46**, 544-549. <https://doi.org/10.1107/S0021889813003531>
- [33] Flores-Gutiérrez, D., Urrutia-Fucugauchi, J., Pérez-Cruz, L., Díaz-Hernández, R. and Linares-López, C. (2010) Scanning Electron Microscopy Characterization of Iron, Nickel and Sulfur in Chondrules from the Allende Meteorite—Further Evidence for between-Chondrules Major Compositional Differences. *Revista mexicana de ciencias geológicas*, **27**, 338-346.
- [34] Gucsik, A., Ott, U., Marosits, E., Karczemska, A., Kozanecki, M. and Szurgot, M. (2008) Micro-Raman Study of Nanodiamonds from Allende Meteorite. *Proceedings of the International Astronomical Union*, **4**, 335-340.
<https://doi.org/10.1017/S1743921308021893>
- [35] Costa, S., Borowiak-Palen, E., Kruszyńska, M., Bachmatiuk, A. and Kaleńczuk, R.J. (2008) Characterization of Carbon Nanotubes by Raman Spectroscopy. *Materials Science Poland*, **26**, 433-441.
- [36] Breitenfeld, L.B., Dyar, M.D., Carey, C.J., Tague, T.J., Wang, P., Mullen, T. and Parente, M. (2018) Predicting Olivine Composition Using Raman Spectroscopy through

- Band Shift and Multivariate Analyses. *American Mineralogist*, **103**, 1827-1836.
<https://doi.org/10.2138/am-2018-6291>
- [37] Avril, C., Malavergne, V., Caracas, R., Zanda, B., Reynard, B., Charon, E., Bobocoiu, E., Brunet, F., Borensztajn, S., Pont, S., *et al.* (2013) Raman Spectroscopic Properties and Raman Identification of CaS-MgS-MnS-FeS-Cr₂FeS₄ Sulfides in Meteorites and Reduced Sulfur-Rich Systems. *Meteoritics & Planetary Science*, **48**, 1415-1426. <https://doi.org/10.1111/maps.12145>
- [38] Taskaev, S., Skokov, K., Khovaylo, V., Donner, W., Faske, T., Dudorov, A., Gorkavyi, N., Savosteenko, G., Dyakonov, A., Baek, W., *et al.* (2019) Pele's Hairs and Exotic Multiply Twinned Graphite Closed-Shell Microcrystals in Meteoritic Dust of Chelyabinsk Superbolide. arXiv: 1905.08003.
- [39] Zega, T. (2004) Serpentine Nanotubes in the Mighei CM Chondrite. *Earth and Planetary Science Letters*, **223**, 141-146. <https://doi.org/10.1016/j.epsl.2004.04.005>
- [40] Liesegang, R. (1907) Ueber einige Eigenschaften von Gallerten. *Zeitschrift für Chemie und Industrie der Kolloide*, 1, Article No. 212.
<https://doi.org/10.1007/BF01830142>
- [41] Bolser, D., Zega, T.J., Asaduzzaman, A., Bringuier, S., Simon, S.B., Grossman, L., Thompson, M.S. and Domanik, K.J. (2016) Microstructural Analysis of Wark-Lovring Rims in the Allende and Axtell CV 3 Chondrites: Implications for High-Temperature Nebular Processes. *Meteoritics & Planetary Science*, **51**, 743-756.
<https://doi.org/10.1111/maps.12620>
- [42] Müller, W.F., Weinbruch, S., Walter, R. and Müller-Beneke, G. (1995) Transmission Electron Microscopy of Chondrule Minerals in the Allende Meteorite: Constraints on the Thermal and Deformational History of Granular Olivine-Pyroxene Chondrules. *Planetary and Space Science*, **43**, 469-483.
[https://doi.org/10.1016/0032-0633\(94\)00181-P](https://doi.org/10.1016/0032-0633(94)00181-P)
- [43] Goldstein, J.I., Scott, E.R.D. and Chabot, N.L. (2009) Iron Meteorites: Crystallization, Thermal History, Parent Bodies, and Origin. *Geochemistry*, **69**, 293-325.
<https://doi.org/10.1016/j.chemer.2009.01.002>
- [44] Tachibana, S. (2006) Chondrule Formation and Evolution of the Early Solar System. *Journal of Mineralogical and Petrological Sciences*, **101**, 37-47.
<https://doi.org/10.2465/jmps.101.37>